



Short communication

Effect of ultracapacitor-modified PHEV protocol on performance degradation in lithium-ion cells

Clark G. Hochgraf^a, John K. Basco^b, Theodore P. Bohn^c, Ira Bloom^{b,*}^a Rochester Institute of Technology, 78 Lomb Memorial Drive, Rochester, NY 14623, USA^b Chemical Sciences and Engineering Division, Argonne National Laboratory, 9700 South Cass Avenue, Argonne, IL 60439, USA^c Energy Systems Division, Argonne National Laboratory, 9700 South Cass Avenue, Argonne, IL 60439, USA

H I G H L I G H T S

- ▶ An ultracapacitor in parallel with a battery was modeled and tested experimentally.
- ▶ The ultracapacitor lowered the energy throughput of the battery.
- ▶ Batteries coupled with an ultracapacitor showed less capacity loss.
- ▶ Batteries coupled with an ultracapacitor showed less resistance growth.

A R T I C L E I N F O

Article history:

Received 19 July 2012

Received in revised form

11 September 2012

Accepted 13 September 2012

Available online 20 September 2012

Keywords:

Lithium-ion battery

Ultracapacitor-battery hybrid

Battery testing

Cycle life

Electric vehicle

PHEV

A B S T R A C T

The cycle life of lithium-ion batteries was investigated using a modified USABC electric vehicle testing protocol designed to simulate the effect of a hybrid energy-storage system (ultracapacitor and battery) in a plug-in hybrid electric vehicle. A side-by-side comparison of battery capacity and impedance changes with and without the effect of the ultracapacitor was performed. Calendar-life degradation effects were corrected for using control cells. The battery's rate of cycle-related capacity degradation decreased by a factor of 2 and rate of cycle-related impedance degradation, by a factor of 5.9 when exposed to the ultracapacitor-modified profile. The modified profile avoids exposure to regeneration energy and reduces maximum voltage of the battery.

© 2012 Elsevier B.V. All rights reserved.

1. Introduction

With their very attractive combination of high specific- and volumetric-power and energy densities, lithium-ion batteries are being considered for use in many types of electric vehicles, such as hybrid, plug-in hybrid, and fully electric vehicles (HEVs, PHEVs, and EVs, respectively). Each vehicle application has a unique set of requirements for the battery, but a common thread among them is long cycle life [1–3]. EV and PHEV applications stress the battery more than the HEV application does because they use a large fraction of the available energy (~80% for an EV, ~50–60% for a PHEV, but ~10% for an HEV). Many ideas have been proposed to lessen the stress on the battery, thereby increasing its life. One such

is to use an ultracapacitor in parallel with a battery to ease the power demands on the battery [4–6]. Here, the ultracapacitor would absorb energy from regenerative braking and assist the battery during discharge. Using an ultracapacitor would be expected to affect the cycle life of a PHEV or EV battery by lessening its energy throughput and peak discharge power. Quantification of this hypothesized effect is the primary goal of this work.

In this study, the effect of an ultracapacitor in parallel with a lithium-ion battery on cycle life was investigated for the PHEV application. Because matching the operating voltage ranges and impedances of a battery and an ultracapacitor is difficult, the ultracapacitor is assumed to be actively connected to the battery with a bi-directional dc/dc converter. The effect of the ultracapacitor on battery voltage and energy throughput was modeled at the Rochester Institute of Technology. The results from the model were used to modify the charge-depleting, dynamic stress test (DST)

* Corresponding author. Tel.: +1 630 252 4516; fax: +1 630 252 4176.

E-mail addresses: ira.bloom@anl.gov, bloom@cmt.anl.gov (I. Bloom).

profile that is used by the U.S. Advanced Battery Consortium (USABC) to test PHEV batteries for cycle life. Side-by-side testing was performed using the DST profiles [2] with and without modification to experimentally determine the difference in degradation rates.

2. Experimental approach

2.1. Modeling

The model battery–ultracapacitor system was designed to reduce the peak discharge power on the battery and to completely absorb the regenerative braking power. In this way, the battery was not exposed to high voltage during regenerative braking events. The system consisted of a series string of battery–ultracapacitor units. Each unit consisted of an ultracapacitor connected in parallel with the battery through a bidirectional dc/dc converter. The capacitance of the ultracapacitor was 195 F at 3.8 V. The total energy of the ultracapacitor system that could be used was 80 W·h (minimum to peak) and its peak power was ~30 kW for both charge and discharge. The round trip efficiency of the ultracapacitor unit was fixed at 87%.

The state-of-charge (SOC) of the ultracapacitor was managed by a set of threshold rules:

- If the vehicle power was all from regenerative braking, the ultracapacitor should absorb it all.
- If the vehicle power was discharge and greater than 22 kW, the battery power was the vehicle discharge power minus 22 kW from the ultracapacitor.
- At the same time, if the SOC of the ultracapacitor was greater than 50%, the ultracapacitor was discharged at the 3-kW rate whenever the vehicle discharge power demand was greater than 3 kW. This was to prevent charge transfer to the battery.
- If the SOC of the ultracapacitor was more than 10 W·h below 50%, charging took place at the 2-kW rate.

This model was implemented in Microsoft® Excel®.

2.2. Testing

Six commercially available, 5-A·h lithium-ion cells were used for this work. The cell chemistry was based on LiMn_2O_4 and graphite. The tests consisted of characterization and calendar- and cycle-life testing using procedures based on those in the USABC Battery Test Manual for Plug-in Hybrid Electric Vehicles [2]. Briefly, the batteries were characterized in terms of their capacities at the C/1 and 10-kW rates at 40 °C. The batteries were also characterized using the hybrid pulse-power characterization test (HPPC) to determine how battery resistance (and power) changes with SOC. The data from the HPPC test were used to calculate a battery size factor (BSF); from the initial HPPC results, the BSF was found to be 316.

After characterization, two batteries were cycled using the baseline DST profile and two, with modifications suggested by the model. Each discharge cycle started from a fully charged battery. Ten percent of the rated capacity was removed at the C/1 rate, and the cell was allowed to rest for 1 h. The discharge continued by repeated application of the respective DST profile. From the test manual, each discharge cycle removed 3.4 kWh of energy, which was scaled by the BSF [2]. In this case, the fixed amount of energy was 3400 W·h/316, or 10.76 W·h. The batteries were recharged according to the manufacturer's recommendations.¹

¹ Charge at the 5-A rate to 4.2 V; for constant-voltage charge at 4.2 V, the current is less than 1.5 A.

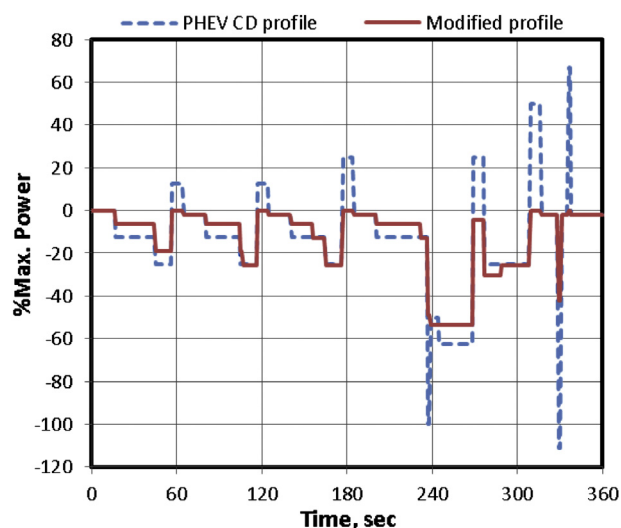


Fig. 1. PHEV profiles used in this work. Discharge is denoted as negative power in the figure.

The remaining two batteries were tested for calendar life so that the net effect of the two cycle-life protocols could be ascertained free of calendar-life effects. These batteries were tested at 60% SOC (~3.92 V) and at 40 °C. Sixty-percent SOC was chosen because it represented an approximate average of the SOC's between which the battery would be cycled.

Every 2 weeks (100 cycles),² testing was stopped and the batteries were characterized by using a reference performance test (RPT). The reference performance test consisted of a capacity measurement at the 10-kW rate and the HPPC test. Testing was then resumed for a total of 5 RPTs, after which the cells could not be cycled due to high cell resistance.

The data from the RPT measurements were collected, normalized to $t = 0$, and averaged. The $t = 0$ points were omitted from all plots and subsequent analyses. For the sake of simplicity, changes in cell performance were gauged in terms of 10-kW-rate capacity and HPPC resistance at 50% SOC (~3.89 V). Plots of these data were then analyzed for trends, using the LINEST function in Microsoft® Excel®.

3. Results

3.1. Modeling

On the basis of results from the model, the PHEV DST profile was modified as shown in Fig. 1. When compared with the baseline profile, also shown in Fig. 1, it can be seen that the modified profile limited the discharge and regeneration power. The large discharge power peaks were lessened and all regeneration (“regen”) power peaks were removed. Here, the stored energy in the ultracapacitor assisted the battery during discharge.

3.2. Testing

The profiles shown in Fig. 1 were repeated during cell discharge. Typically, six repetitions were used to remove 10.76 W·h. Figs. 2 and 3 show the voltage response of the cells to the discharge profiles shown in Fig. 1. From Figs. 2 and 3, the two voltage

² 1 cycle = discharge 10.76 W·h of energy plus recharge. Accumulating 100 cycles took 2 weeks.

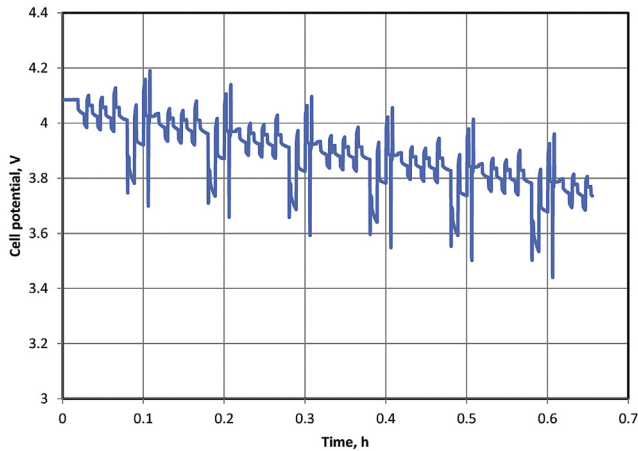


Fig. 2. Cell potential vs. time, showing the voltage response of the cell during discharge using the baseline profile.

responses were different. Comparing Figs. 2 and 3 shows that the discharge process in Fig. 3 is slightly longer than that shown in Fig. 2. The baseline profile (Fig. 2) contained regen power steps, so energy was put into the battery, resulting in a slightly longer discharge process to remove a fixed amount of energy. The modified profile also limited the change in cell voltage at each point during discharge.

3.2.1. Effect of cycling profile on capacity fade

As expected, cell capacity decreased with time and cycle count. A plot of the change in the average relative capacity values for the cells tested with the baseline and modified profiles, along with those from the calendar-life test, is given in Fig. 4. The plot shows that the calendar-life cells displayed the smallest change in relative capacity, and those cycled with the baseline profile, the greatest. The total capacity losses using the baseline and modified profiles were 30 and 22%, respectively. Indeed, the total capacity loss displayed by the cells cycled with the modified profile was only slightly larger than that shown in the calendar-life test, 19%.

A least-squares regression analysis of the data in Fig. 4 shows that capacity decline followed two kinetic rate laws, $at^{1/2} + b$ in the calendar-life test and $at + b$ in the cycle-life test. The values of the fitting parameters and the regression coefficients are given in

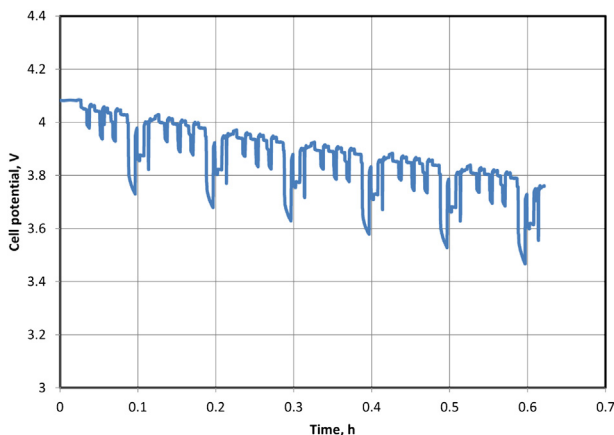


Fig. 3. Cell potential vs. time, showing the voltage response of the cell during discharge using the modified profile.

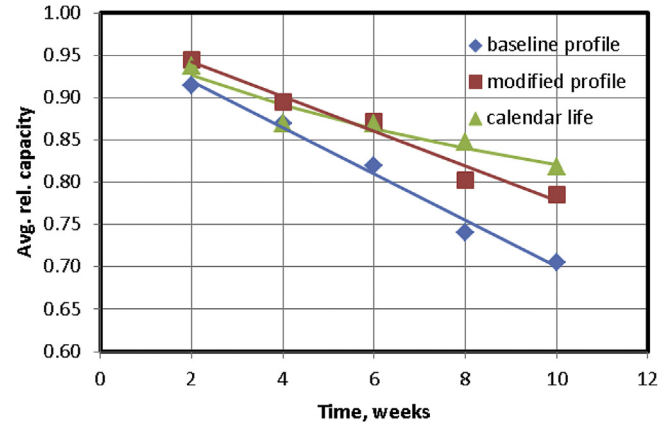


Fig. 4. Average, relative 10-kW-rate capacity vs. time. The data are shown as points, and the least-squares fit to the data, as solid curves.

Table 2, along with the kinetic law used. From the data in Table 1, the fits were good, with values of r^2 of 0.91 or better. Comparing the values of a for the two cycle-life tests shows that rate of capacity loss using the modified profile was approximately 75% of that when using the baseline profile.

Using the fits of Table 1 and assuming that the contributions of cycling and calendar time combine linearly, we recalculated the data shown in Fig. 4, removing the effect of calendar time. These data are shown in the plot in Fig. 5. Because the calendar- and cycle-life degradation processes follow different rate laws (see Fig. 4 and Table 1), the curve from the modified profile displayed an apparent increase in capacity (less capacity loss). Comparing the curves in Fig. 5 shows that the net effective capacity fade using the modified profile was less than that from the baseline profile by a factor of about 3. A least-squares analysis of the data in Fig. 5 shows that they could be fitted to the equation, $at + b$, with values of r^2 of 0.96 or better. Inserting the values for the fitting parameters into this equation yields $-1.41 \times 10^{-2}t + 2.56 \times 10^{-2}$ and $-7.29 \times 10^{-3}t + 3.48 \times 10^{-2}$, respectively, for the data from the baseline and modified profiles. The standard deviations for each value in both equations were (a, b) 8.72×10^{-4} and 5.79×10^{-3} . The values of a in these equations show that the rate of capacity loss was slower using the modified profile than using the baseline profile by about a factor of 2.

3.2.2. Effect of cycling profile on resistance

As expected, cell resistance increased with test time and cycle count. A plot of the change in the average relative resistance values is given in Fig. 6 for the three tests in this study. In these tests, the net increases in cell resistance were 75%, 26%, and 20%, respectively, for the baseline profile, the modified profile, and the calendar-life test.

All of the data shown in Fig. 6 were fitted to the equation $at + b$. The values of the fitting parameters and regression coefficients are given in Table 2. From the data in Table 2, the fits were good, with values of r^2 of 0.94 or better. Also from the data in Table 2, the value of a for the modified profile was approximately 44% of that for the

Table 1
Fitting constants and regression coefficients using the data shown in Fig. 4.

Test type	Kinetic law	$10^2 a$ (s.d.)	b (s.d.)	r^2
Calendar life	$at^{1/2} + b$	-6.11 (1.08×10^{-2})	1.01 (2.65×10^{-2})	0.91
Baseline profile	$at + b$	-2.73 (1.73×10^{-3})	0.97 (1.15×10^{-2})	0.99
Modified profile	$at + b$	-2.05 (2.07×10^{-3})	0.98 (1.37×10^{-2})	0.97

Table 2

Fitting constants and regression coefficients using the data shown in Fig. 6.

Test type	$10^2 a$ (s.d.)	b (s.d.)	r^2
Calendar life	2.95 (4.18×10^{-3})	0.89 (2.77×10^{-2})	0.94
Baseline profile	8.90 (3.18×10^{-3})	0.86 (2.11×10^{-2})	0.99
Modified profile	3.96 (3.25×10^{-3})	0.89 (2.15×10^{-2})	0.98

baseline profile. Thus, the rate of resistance increase was smaller using the modified profile.

Again, using the fits and assuming that the contributions from calendar time and cycling time combine linearly, the contributions to resistance increase from calendar time were subtracted, yielding cycling-only contributions to resistance increase. The results of this subtraction are shown in Fig. 7. A least-squares regression of the data in Fig. 7 showed that they could be fitted to the linear-with-time equation, $at + b$, with values of r^2 of 0.99 or better. Indeed, putting the fitted values into this equation yields $5.96 \times 10^{-2}t - 2.84 \times 10^{-2}$ and $1.01 \times 10^{-2}t - 1.70 \times 10^{-2}$, respectively, for the data from the baseline and modified profiles. The standard deviations for both a and b were less than 10^{-9} in both equations. From these results, the net resistance increase rate using the baseline profile was about 5.9 times greater than that from using the modified profile.

3.2.3. Effect of cycling profile on energy efficiency

The effects of the tests on the average, relative energy efficiencies are shown in Fig. 8. In this plot, efficiency is defined as (watt-hours discharged in current cycle)/(watt-hours recharged in next cycle). That is, the recharge came after discharging the cell completely. After completing 100 DST cycles to $\sim 30\%$ SOC, the cells were immediately recharged to 100% SOC, followed by a full discharge and full recharge.

From Fig. 8, we see that there was no significant change in energy efficiency during the calendar-life test. There was a decrease in energy efficiency with time for the cycled cells, with the baseline case being the worst. The calendar-life cells displayed no change in energy efficiency, whereas that of the baseline cycled cells decreased $\sim 7\%$ and the modified profile cells decreased $\sim 2\%$.

4. Discussion

On the basis of Figs. 1–3, the ultracapacitor-modified PHEV profile limited the exposure of the cells to high voltage. Additionally, the modified profile also limited the discharge power demands placed on the cells. The cells tested with this profile exhibited less performance decline than did those tested with the baseline profile.

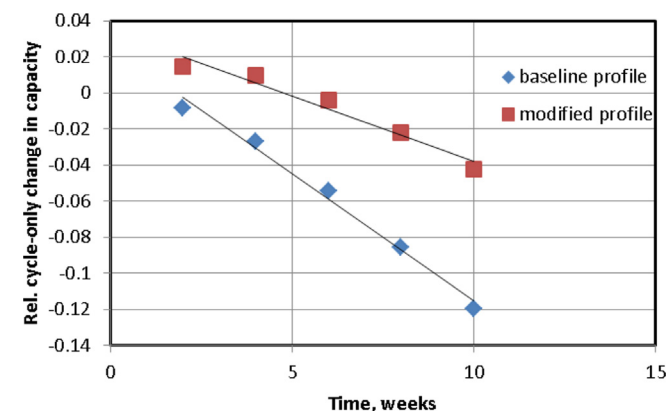


Fig. 5. Data shown in Fig. 4 with the contributions from calendar time removed.

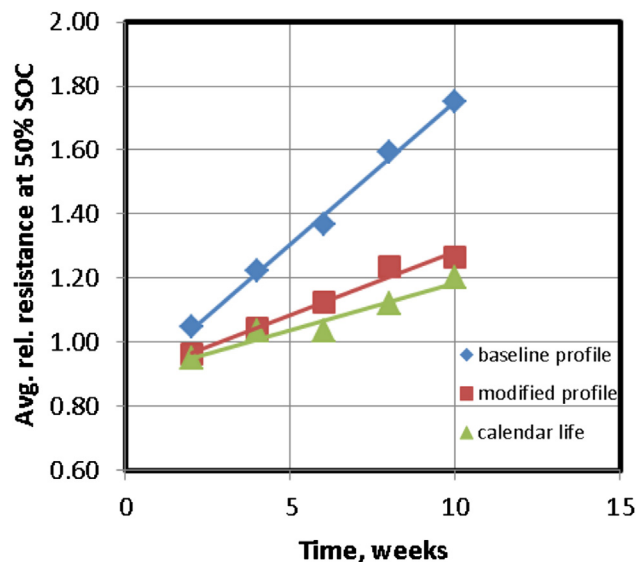


Fig. 6. Average relative resistance at 50% SOC vs. time. The data are shown as points, and the least-squares fit to the data, as solid curves.

The test profiles changed both the total performance decline and the rate at which it declined. This was seen in terms of capacity, resistance, and energy efficiency change. For example, using the calendar-time-free results, the cells tested with the baseline profile exhibited three times the capacity loss of those tested with the modified profile and reached that level of performance decline approximately twice as fast.

The effects of the modified profile on net resistance increase and the rate of increase were even more striking. Here, the differences were on the order of a factor of 6. The total resistance increase was higher and the rate of increase was faster using the baseline profile than using the modified one.

The effect of the cycling profile was also seen in the changes in energy efficiency of the cell. Here, the effect was smaller in the absolute sense than the other effects observed. Relatively speaking, however, the modified profile energy efficiency losses were a factor of about 3 smaller than that of the baseline profile.

There are many possible reasons for the observed effect on performance parameters. For example, there are differences in the

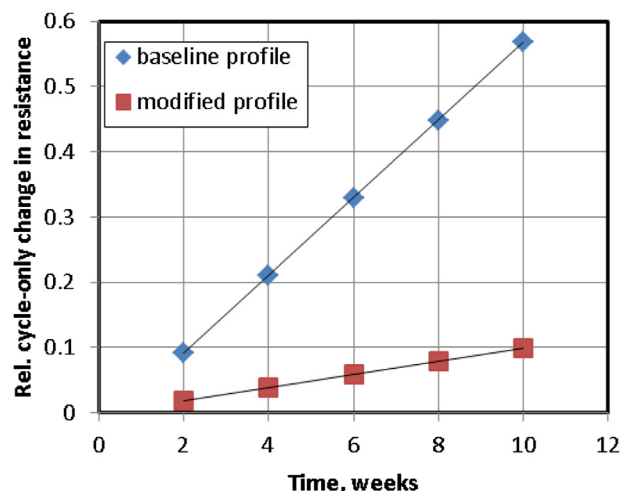


Fig. 7. Data shown in Fig. 6 with the contributions from calendar time removed.

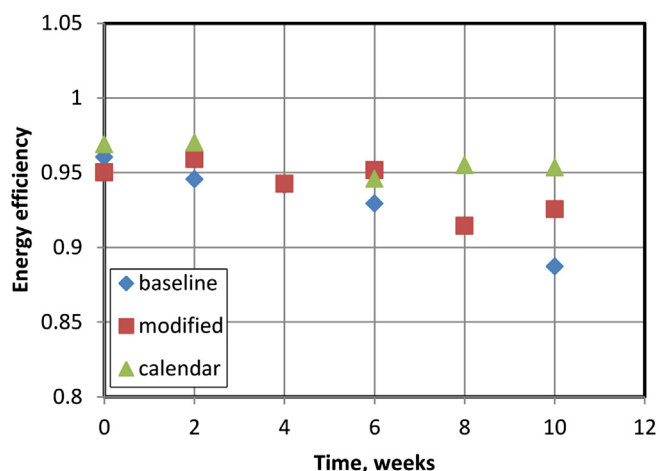


Fig. 8. Average energy efficiency of the cells vs. time.

Table 3

Unscaled, discharge peak power and net energy throughput using two cycling profiles.

Profile name	Discharge peak power, kW	Discharge energy, W·h	Charge energy, W·h
Baseline	50	687.28	141.67
Modified	24	563.57	0.00

discharge peak power and discharge and regeneration energy throughputs using the baseline and modified profiles. These parameters are given in Table 3. From these data, the peak power demands imposed by the modified profile are about a factor of 2 less than those from the baseline. With less power demand, there would be less heating and, thus, fewer heat-induced changes in cell performance. Additionally, since an ultracapacitor is used, the modified profile also demands less energy throughput on discharge and charge from the cell. The energy throughput of the modified profile is about 82% of that of the baseline during discharge and 0% during charge.

With no charge energy in the ultracapacitor-modified profile, the cell was not charged to high voltages. Time at high voltages has been reported to be detrimental to the performance of many cell chemistries, leading to enhanced capacity fade and resistance increase [7–14]. Thus, using an ultracapacitor can, potentially, increase the life of the cell.

5. Conclusion

The cycle life of full-sized, lithium-ion batteries based on LiMn_2O_4 and graphite was investigated using the USABC PHEV profile and a modified protocol designed to simulate the effect of an energy storage system consisting of an ultracapacitor in parallel with a battery in a plug-in hybrid electric vehicle. The modified profile avoids exposure to regeneration energy and reduces maximum voltage of the battery. A side-by-side comparison of battery capacity and impedance changes with and without the effects of the ultracapacitor was performed. Calendar-life degradation effects were corrected for by using control cells. The results were consistent between replicates. The battery's rate of cycle-related capacity degradation was decreased by a factor of 2 and cycle-related impedance degradation, by a factor of 5.9 when exposed to the ultracapacitor-modified PHEV profile.

Acknowledgment

The work at Argonne National Laboratory was performed under the auspices of the U.S. Department of Energy, Office of Vehicle Technologies, Hybrid and Electric Systems, under Contract No. DE-AC02-06CH11357.

References

- [1] FreedomCAR Battery Test Manual for Power-Assist Electric Vehicles, DOE/ID-11069, October 2003.
- [2] Battery Test Manual for Plug-In Hybrid Electric Vehicles, INL/EXT-07-12536, Rev. 2, December 2010.
- [3] Electric Vehicle Battery Test Procedures Manual, Rev. 2, January 1996.
- [4] M. Ortúzar, J. Moreno, J. Dixon, IEEE Transactions on Industrial Electronics 54 (4) (August 2007) 2147–2156.
- [5] R.A. Dougal, S. Liu, R.E. White, IEEE Transactions Component Packaging Technology 25 (1) (March 2002) 120–131.
- [6] A. Burke, M. Miller, H. Zhao, EVS-25, Shenzhen, China, Nov. 5–9, 2010.
- [7] R.G. Jungst, G. Nagasubramanian, H. Case, A. Urbina, T.L. Paez, D.H. Doughty, in: G.A. Nazri, E. Takeuchi, B. Scrosati (Eds.), Electrochemical Society Series, International Symposium on Batteries and Supercapacitors, San Francisco, CA, 2001, 85–95 (pub. 2003).
- [8] R.B. Wright, C.G. Motloch, J.R. Belt, J.P. Christophersen, C.D. Ho, R.A. Richardson, I. Bloom, S.A. Jones, V.S. Battaglia, G.L. Henriksen, T. Unkelhaeuser, D. Ingersoll, H.L. Case, S.A. Rogers, R.A. Sutula, Journal of Power Sources 110 (2002) 445–470.
- [9] K. Amine, C.H. Chen, J. Liu, M. Hammond, A. Jansen, D. Dees, I. Bloom, D. Vissers, G. Henriksen, Journal of Power Sources 97–98 (2001) 684–687.
- [10] J. Belt, V. Utgikar, I. Bloom, Journal of Power Sources 196 (2011) 10213–10221.
- [11] M. Broussely, S. Herreyre, P. Biensan, P. Kasztejna, K. Nechev, R.J. Staniewicz, Journal of Power Sources 97–98 (2001) 13–21.
- [12] M.-S. Wu, P.-C. Chiang, J.-C. Lin, Journal of the Electrochemical Society 152 (2005) A1041–A1045.
- [13] R.P. Ramasamy, R.E. White, B.N. Popov, Journal of Power Sources 141 298–306.
- [14] X. Wang, H. Nakamura, M. Yoshio, Journal of Power Sources 110 (2002) 19–26.